Journal of Theoretical Biology 298 (2012) 32–41

Contents lists available at SciVerse ScienceDirect

Journal of Theoretical Biology

journal homepage: www.elsevier.com/locate/yjtbi

Strategies for cancer stem cell elimination: Insights from mathematical modeling

Vladimir Vainstein*, Oleg U. Kirnasovsky, Yuri Kogan, Zvia Agur

Institute for Medical Biomathematics, 10 Te'ena str, P.O.B. 282, 60991 Bene Ataroth, Israel

ARTICLE INFO

Article history:
Received 9 March 2011
Received in revised form
29 September 2011
Accepted 15 December 2011
Available online 23 December 2011

Keywords:
Cellular automata
Cell differentiation
Cancer therapy

ABSTRACT

The cancer stem cell (CSC) hypothesis states that only a small fraction of a malignant cell population is responsible for tumor growth and relapse. Understanding the relationships between CSC dynamics and cancer progression may contribute to improvements in cancer treatment. Analysis of a simple discrete mathematical model has suggested that homeostasis in developing tissues is governed by a "quorum sensing" control mechanism, in which stem cells differentiate or proliferate according to feedback they receive from neighboring cell populations. Further analysis of the same model has indicated that excessive stem cell proliferation leading to malignant transformation mainly results from altered sensitivity to such micro-environmental signals. Our aim in this work is to expand the analysis to the dynamics of established populations of cancer cells and to examine possible therapeutic avenues for eliminating CSCs. The proposed model considers two populations of cells: CSCs, which can divide indefinitely, and differentiated cancer cells, which do not divide and have a limited lifespan. We assume that total cell density has negative feedback on CSC proliferation and that high CSC density activates CSC differentiation. We show that neither stimulation of CSC differentiation nor inhibition of CSC proliferation alone is sufficient for complete CSC elimination and cancer cure, since each of these two therapies affects a different subpopulation of CSCs. However, a combination of these two strategies can substantially reduce the population sizes and densities of all types of cancer cells. Therefore, we propose that in clinical trials, CSC differentiation therapy should only be examined in combination with chemotherapy. Our conclusions are corroborated by clinical experience with differentiating agents in acute promyelocytic leukemia and neuroblastoma.

1. Introduction

The theory of cancer stem cells (CSCs) has drawn substantial attention from the scientific community in recent years (Sell, 2004; Zhou et al., 2009). According to this theory, cancer progression is governed by CSCs, a subset of stem cell-like tumor cells that have the potential for unlimited replication and tumor initiation. The majority of tumor cells, in contrast, can undergo only a limited number of divisions and therefore cannot repopulate a depleted tumor. Research findings are as yet inconclusive with regard to the universal applicability of the CSC theory (Quintana et al., 2008, for example, found evidence of a relatively large tumorigenic population among human melanoma cells, potentially challenging the CSC hypothesis for this type of cancer; see also Tomasson, 2009; Adams and Strasser, 2008; Kelly et al., 2007). Nonetheless, CSCs have been found to play crucial roles in the development and progression of leukemias and different solid tumors (le Viseur et al., 2008; Kavalerchik et al., 2008; Boman and Huang, 2008; Pohl et al., 2008; Kakarala and Wicha, 2008).

The CSC paradigm holds meaningful ramifications for cancer therapy. As even a few CSCs might be sufficient to generate a tumor, one can intuitively conclude that an effective treatment must target the CSC population, ensuring that it dies out or at least does not manage to expand. Studies suggest that CSCs are relatively resistant to standard cytotoxic therapies (Cortes-Dericks et al., 2010). Therefore, there have been attempts to develop compounds that induce differentiation of CSCs in order to eliminate their ability to proliferate indefinitely, effectively exterminating cancer (Sanchez-Garcia et al., 2007; Spira and Carducci, 2003). Yet thus far, despite considerable research efforts and promising results in *in vitro* studies (see Spira and Carducci, 2003; Sell, 2004 for review), differentiation therapy has shown consistent clinical effectiveness for only one cancer indication: acute promyelocytic leukemia. Notably, in all clinical trials in which differentiating agents were administered as monotherapy, treatment either was of no efficacy at all (Trump et al., 1997; Culine et al., 1999; Adamson et al., 2007; Iida et al., 1999) or

* Corresponding author. Tel.: +972 39733075; fax: +972 39733410.
E-mail addresses: vladimir.dr@gmail.com, vladimir@imbm.org (V. Vainstein), oleg_kirnasovsky@mail.ru (O.U. Kirnasovsky), yuri@imbm.org (Y. Kogan), agur@imbm.org (Z. Agur).

0022-5193/$ - see front matter © 2011 Elsevier Ltd. All rights reserved.
doi:10.1016/j.jtbi.2011.12.016

produced only a delay in relapses (Studer et al., 1995). However, the combination of differentiation therapy with chemotherapeutic agents was efficacious both in acute promyelocytic leukemia (Rowe and Tallman, 2009), for which it has become a standard of care, and more recently in neuroblastoma (Matthay et al., 2009).

There are different potential factors underlying the low efficacy observed in clinical trials of cytotoxic therapy and of differentiation therapy targeting CSC populations. Regular cytotoxic therapies generally affect rapidly proliferating cells, whereas evidence suggests that only a small fraction of CSCs actively proliferate, indicating an inherent resistance of the CSC population to this type of therapy (Cortes-Dericks et al., 2010). Another factor could be toxicity, which poses restraints on dosage and thus might limit treatment scope and effect. A third reason might stem from the intricate dynamics governing cancer cell populations, particularly populations characterized by a hierarchical structure. The typical response of a single cell to treatment cannot be easily generalized in order to predict the response of an entire cell population. Rather, the macroscopic behavior of cancerous tissue emerges from the combination of individual cell–cell interactions, driven by global and local feedback. The death or differentiation of one cell as a result of therapy may trigger or inhibit a nearby cell's transition between a quiescent state and a proliferative state, or from a stem state to a differentiated state, thereby influencing its susceptibility to treatment. Thus, for example, mass induction of cell death or CSC differentiation might set off complex processes that prevent the CSC population from being eliminated, or even stimulate its growth.

In light of the above, it is necessary to gain a deeper understanding of how a cancer cell population is affected by different types of CSC-based therapy, both alone and in combination with other types of interventions. As noted by Flake (2004), systems biology tools may be very useful in the analysis of the complex dynamics of CSCs. Such tools can help researchers to investigate different properties of CSC dynamics reflected in cancer progression, and to learn how to influence these properties in order to control or eradicate tumors.

As early as Tomlinson and Bodmer (1995) modeled cancer in the context of stem cell hierarchy; they considered a normal stem cell-driven cell population and investigated possible factors contributing to malignant transformation. When the CSC hypothesis began to take root, modeling efforts extended in several directions. Some researchers pursued generic questions about how hierarchical population structure affects tumor transformation and progression, including questions regarding the regulation of CSC division and differentiation (e.g., Ganguly and Puri, 2006; Bankhead et al., 2007; Boman et al., 2007; Sottoriva et al., 2010; Zhu et al., 2011). Others examined the effects of tumorigenic mutations in different compartments of hierarchical populations (e.g., Michor et al., 2003; Dingli et al., 2007; Ashkenazi et al., 2007), and some modeled CSC migration and investigated its effects on tumor invasiveness and heterogeneity (e.g., Enderling et al., 2009a, 2009b, 2010; Sottoriva et al., 2010). Additional studies focused on specific cancer types, including hematopoietic cancer (Dingli and Michor, 2006; Abbott and Michor, 2006) and colorectal cancer (Johnston et al., 2007; van Leeuwen et al., 2007; d'Onofrio and Tomlinson, 2007).

Some of these mathematical models have also been used to investigate questions of therapy under the CSC hypothesis. Such studies have consistently shown that treatment should specifically target the CSC subpopulation. In particular, they suggest that therapies that affect cells indiscriminately in order to reduce CSC load may be detrimental (Boman et al., 2007; Dingli and Michor, 2006; Enderling et al., 2009a, 2009b; Zhu et al., 2011; Sottoriva et al., 2010).

Herein we propose a mathematical model to investigate how tumor progression is affected by differentiation therapy and by standard (cytotoxic or antiproliferative) therapy, both alone and in combination. To our knowledge, this question has not been directly examined thus far with the aid of mathematical models. To increase the generality of our conclusions, we rely on a minimum of assumptions, i.e., our model is not dependent on specific tissue characteristics or drug mechanisms of action. To accurately capture the emergent tissue dynamics, we use a cellular automata (CA) model that is driven by local cell–cell interactions, yet ultimately provides an indication of tissue response at a population level (see, e.g., Moreira and Deutsch, 2002 for a review of CA application to tumor modeling).

In previous studies, we formulated CA models, based on minimal assumptions, that captured stem cell dynamics in a tissue. These models incorporated local control of stem cell fate (Agur et al., 2002, 2010; Kirnasovsky et al., 2008a). We used this modeling approach to demonstrate that "quorum sensing" of stem cells – i.e., direct stimulation of differentiation of a stem cell by its neighboring stem cells – is sufficient for maintaining tissue homeostasis (Agur et al., 2010). Moreover, the range of a cell's quorum sensing capacity, i.e., the distance at which the cell is able to receive feedback from its neighbors, was found to be the most influential parameter governing the transition from tissue homeostasis to uncontrolled malignant growth. Indeed, local control by interaction with the microenvironment is being established as a major mechanism of normal stem cell regulation and a probable point of derangement in CSCs (Kirouac et al., 2009).

Continuing our previous work (Agur et al., 2002, 2010; Kirnasovsky et al., 2008a), here we use a CA model based on biologically plausible assumptions regarding solid tumors characterized by a hierarchical structure (e.g., breast and colon). Simulation results show that anti-proliferation therapy and treatment promoting differentiation are each ineffective when administered alone. Rather, we find that only treatment that simultaneously prevents CSC proliferation and promotes differentiation can effectively eliminate CSCs and lead to tumor eradication. We propose, therefore, that future research should focus on therapy that targets CSC proliferation and differentiation simultaneously, rather than on either of these options alone.

2. Methods

2.1. Model assumptions

The model describes two subpopulations of cancer cells in a growing tumor: CSCs and differentiated cancer cells (DCs). Our approach is based on principles similar to those we used in previous studies (Agur et al., 2002; Kirnasovsky et al., 2008a; Agur et al., 2010), namely, the assumption of local control of cell fate (quorum sensing). In contrast to previous models, however, this model describes cell behavior in stochastic terms. We assume that each CSC is either "non-cycling" (quiescent, a state that can be maintained for any period of time) or "cycling", i.e., the cell progresses through the cell cycle and after a fixed time period divides into two CSCs. Non-cycling CSCs can enter the cell cycle at any time. The "decision" of a non-cycling CSC to enter the cell cycle is controlled by the total cell density in the CSC's vicinity: the more vacant (i.e., unoccupied by other cells) space available, the greater the probability that the CSC will enter the cell cycle. In addition, non-cycling CSCs can undergo differentiation and become DCs. The decision of a non-cycling CSC to differentiate is controlled by the local density of CSCs: the probability that a CSC will differentiate increases with the number of its CSC neighbors. This type of dependence reflects our major assumption, that local cell–cell feedback regulates proliferation and differentiation decisions. This assumption, operationalized as

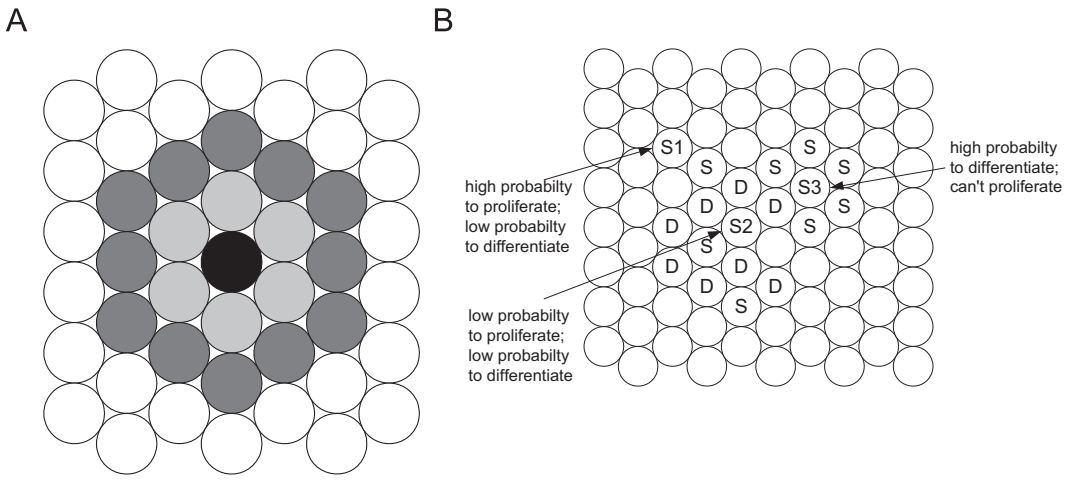

Fig. 1. An illustration of the CA structure, definition of neighborhood and CSC regulation. (A) The cells of the CA are circles tightly positioned on the plane. The six cells adjacent to a central (black) cell are first-degree neighbors (marked in light grey). The 12 second-degree neighbors are marked in a darker grey. (B) Illustrative examples of CSC decisions. A CSC marked as *S1* has only one stem neighbor (marked as *S*); therefore it is not likely to differentiate and has a relatively high probability to enter the cell cycle. The CSC marked as *S2* is mostly surrounded by DCs (marked as *D*); therefore it also has low probability to differentiate, but also low probability to enter the cycle (having only one vacant adjacent site). The CSC marked as *S3* is mostly surrounded by CSCs (marked by *S*) and thus has higher probability differentiate, but cannot enter cell cycle, until the adjacent DC dies.

the quorum sensing mechanism, is consistent with biological observations that cell differentiation is driven by feedback from the microenvironment (e.g., Clarke et al., 2003). This feedback might come from direct contact between CSCs, or it may result from other factors in the microenvironment that regulate CSC expansion according to local cell density (such as paracrine signaling, niche availability, etc.). Furthermore, we assume that DCs do not proliferate and have a constant lifespan, at the end of which they die and disappear.

2.2. Formal description of the model

The model is implemented by generalized probabilistic CA. The base set of the CA is the set

$$G = \{\langle x,y\rangle \in \mathbb{Z}_{100} \times \mathbb{Z}_{100} \,|\, x \equiv y (\mathrm{mod}\ 2)\}.$$

In order to prevent confusion we will hereafter refer to the virtual cells of the automata as "automata cells", as opposed to "cells", which refers to the living cells being modeled. Each automata cell $\langle x,y\rangle$ has exactly six neighbors: $\langle x-2,y\rangle$, $\langle x-1,y-1\rangle$, $\langle x-1,y+1\rangle$, $\langle x+1,y-1\rangle$, $\langle x+1,y+1\rangle$ and $\langle x+2,y\rangle$, where addition and subtraction are in the quotient ring $\mathbb{Z}_{100}$. The structure of the neighborhood is isomorphic to that of equal spheres that are tightly disposed on the plane,[1] and it constitutes a close approximation of tightly distributed cells (see Fig. 1A). Closing of each of two directions by means of the notion of a quotient ring corresponds to the closing of a plane rectangle onto a torus surface.

The model proceeds by discrete time steps. At a given time step, each automata cell contains either a single cell or a vacant space. The state of each automata cell at each time step consists of the following variables, as applicable:

(a) the type of automata cell (a non-cycling CSC, a cycling CSC, a DC, or an empty space);
(b) the age (for a DC);
(c) the stage of progression through the cell cycle (for a cycling CSC).

The initial state of the model comprises the states of all automata cells at time zero. To simulate the model, a random ordering on the set G is chosen. At each discrete time step, the automata cells undergo several sequential stages of processing according to the following rules. At each stage, all automata cells are processed one after the other, according to the predetermined order. In the first stage, each cell is processed for the decision of DC death; each DC that dies is replaced with an empty space. Next, each cell is processed for the decision of CSC differentiation; each CSC that differentiates is replaced with a DC. Then, each cell is processed for the decision of non-cycling CSCs to enter the cell cycle. The ability of a CSC to enter the cell cycle is contingent on the availability of a neighboring empty space into which the CSC will later be able to divide. Then, every cycling cell that has reached the final step of the division stage of the cell cycle turns into two non-cycling CSCs. When a CSC divides, one of the two daughter cells remains in the site of the original CSC, and the other moves into a neighboring empty site. In order to prevent the same site from being occupied by two newborn cells, when a CSC enters the cell cycle, one of its empty neighboring automata cells is randomly chosen to be reserved for one of the daughter cells. All other CSCs subsequently consider the reserved automata cell to be non-empty, and thus they are unable to divide into it. In the final stage of processing, the counters for the ages of DCs and for the cell cycle progression of cycling CSCs are increased by one.

The CSC differentiation and proliferation decision processes are formally implemented in the model as follows.

CSC differentiation decision: If A is a non-cycling CSC in our model, we calculate the weighted number ("density") of CSCs in its neighborhood:

$$den(A) = N_1 + \frac{N_2}{2k},$$

where N_1 is the number of first-degree CSC neighbors of A, i.e., neighboring automata cells occupied by CSCs; N_2 is the number of second-degree CSC neighbors, i.e., the automata cells that are neighbors of A's neighbors (but are not A's first-degree neighbors) and are occupied by CSCs; k is the damping coefficient that

[1] The most famous example of this structure in nature is the honeycomb. An isomorphism can be realized by the mapping $\langle x,y\rangle \mapsto \langle xR\sqrt{3}, yR\rangle$, where R is the radius of the equal spheres.

reduces the effect of the second-degree neighbors. Then, the probability p_d of the cell A to differentiate at the current time step is determined by a sigmoid-like function:

$$p_d = p_{\max} - \frac{a^m (p_{\max} - p_{\min})}{a^m + (den(A))^m}.$$

Here $p_{\min}$ is the minimal probability of differentiation (reached when the number of neighboring CSCs is zero), $p_{\max}$ is the maximal probability of differentiation (reached when the number of neighboring CSCs is infinite), hereafter termed "maximal differentiation rate", a is the CSC density in the neighborhood that gives the probability $0.5 \cdot (p_{\min} + p_{\max})$, and m is function steepness. In this work, $p_{\min}$ was set to zero and m to 5.

CSC decision to enter the cell cycle: The probability of a non-cycling CSC to enter the cell cycle at a given time step is calculated as follows:

$$p_c = 1 - (1 - p_0)^n = np_0 + o(p_0),$$

where n is the number of vacant automata cells in the neighborhood of a given cell, calculated similar to $den(A)$, and p_0 is a parameter, representing the basic probability to enter the cell cycle (i.e., the probability to enter the cycle when only one empty neighboring automata cell is available), hereafter referred to as the "proliferation rate". As noted above, upon the decision of a cell to enter the cell cycle, one of its adjacent empty automata cells is chosen randomly to be reserved for one of its future daughter cells. If there are no empty non-reserved automata cells in the neighborhood, the cell remains a non-cycling CSC. The structure of the neighborhood in our model and illustrative examples of CSC decision rules are shown in Fig. 1. A flowchart summarizing the decision process for cells of different types is shown in Fig. 2.

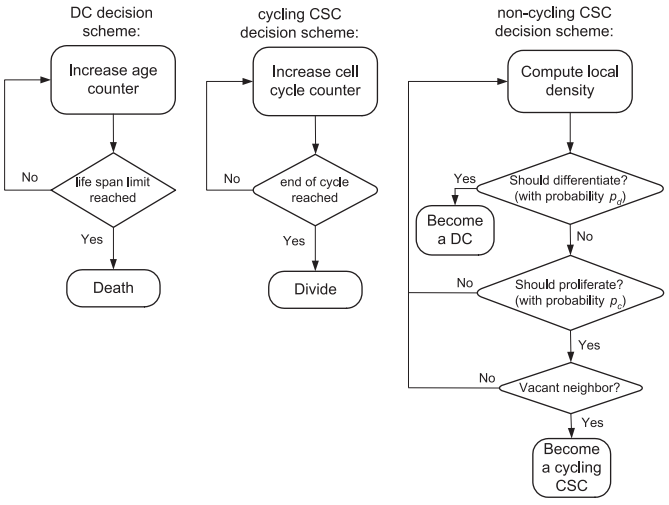

Fig. 2. A flowchart of cell decisions in the model. We summarize the decision taken by each type of cells (DC, cycling CSC, non-cycling CSC) during the automata run. The scheme is repeated at each time step for each cell.

2.3. Computer simulations

All the algorithms were implemented in C++. We started all simulations from a given number of cells, a given percent of which were DCs whose ages were chosen randomly with uniform distribution on an interval of possible ages, while the other cells were non-cycling CSCs. At time zero all cells were randomly positioned in a subsquare of a given size of the base square $\mathbb{Z}_{100} \times \mathbb{Z}_{100}$. We set the discrete time step in the simulations to 30 min. Every simulation was run for 20,000 steps; thus, the corresponding time of the development of each cell colony was equal to 10,000 h. This amount of time was observed to be long enough for the model to reach a quasi-steady state (a state with an approximately constant number of cells of each type over time in the whole CA) for all initial conditions and parameter values studied (Table 1).

2.4. Parameter values

Direct *in vivo* measurements of kinetic parameters of CSC proliferation and differentiation are currently unavailable. Therefore, we used published indirect estimates where available (Table 1). The reported proportions of apoptotic tumor cells in different human solid tumors are 0.5−10%, as measured by the TUNEL technique, which stains cells in the last phase of apoptosis (i.e., DNA fragmentation), lasting up to a few hours (Lipponen, 1999; Sinicrope et al., 1999). Taking the representative value of 1% and assuming the duration of the apoptosis phase measured by TUNEL was 2 h, we roughly estimated the average lifespan of DCs to be 50 h, with a range of 30–180 h. In most human solid tumors, the mitotic index varies in the range of 1−20%, with a mitosis duration of 1–2 h (Lipponen, 1999; Sinicrope et al., 1999). Consequently, the proportion of cells entering the cell cycle can be estimated in the range 0.005–0.2 per hour. To effectively sample the biologically plausible range, we assumed minimal value of the basic probability to enter the cell cycle to be 0.0015 and each subsequent value twice the previous, up to 0.048 (recall that the actual probability equals the basic probability times the number of vacant automata cells in the neighborhood). The values for the differentiation rate of CSCs are especially difficult to estimate from the literature. For the maximum differentiation rate, p_{max}, we used a wide range, 0.025−0.8 per hour.

Table 1
Model parameters and initial conditions. Values of the parameters and initial conditions are specified. The parameter estimation is detailed in Section 2.4. For analysis of model sensitivity to stochastic effects and initial conditions, the values from the third column were used. For the analysis of the model dynamics under different parameter values, the parameters and initial conditions values from the fourth column were used.

List of parameters and initial conditions	Baseline values	Values for analysis of model sensitivity	Values for analysis of parameter variation
Lifespan of DC (hours)	90	30, 60, 90, 120, 150, 180	30, 60, 90, 120, 150, 180
Damping coefficient for the second degree neighbors, k	2	2	1.25, 1.5, 1.75, 2, 2.25 , 2.5
Basic probability of entering cell cycle, p_0	0.006	0.006	0.0015, 0.003, 0.006, 0.012, 0.024, 0.048
Maximal differentiation rate, p_{max}	0.1	0.1	0.025, 0.05, 0.1,0.2, 0.4, 0.8
Number of CSC neighbors giving the half-maximal differentiated rate, a	3	2, 2.5, 3, 3.5, 4, 4.5	2, 2.5, 3,3.5, 4, 4.5
Initial cell number	100	10, 100, 1000, 3000	100
Initial percentage of DC	30	0, 10, 20, 30, 40, 50	30
Size of subsquare of initial cell distribution	20×20	6×6, 20×20, 60×60, 100×100	20×20
Minimal and maximal age of initial DC subpopulation (as a fraction of DC lifespan)	(0;1)	(0;0.1), (0;0.5), (0.9;1), (0;1)	(0;1)

These values correspond, respectively, to 2.5−80% of CSCs undergoing differentiation within 1 h if fully surrounded by other CSCs. For the value of local CSC density needed to reach the half-maximal rate of differentiation, a, we used the range 2–4.5, given that in the model each cell can have up to six immediate neighbors. The duration of the cell cycle (defined here as the time between the restriction point in G1 until the end of M-phase) was set at 12 h. We assumed that the cell cycle duration for CSCs was 12 h (Salmon and Sartorelli, 2001).

We defined a set of "baseline" kinetic parameter values as the values in the middle of the estimated ranges, as well as a set of baseline initial conditions. Initial conditions included the initial number of cells, the initial percentage of DCs, the initial size of the subsquare, and the minimum and maximum ages of the initial DC subpopulation.

3. Results

We first attempted to characterize the model's general behavior under different conditions. To this end we carried out 100 simulations for each of 13,824 combinations of different initial conditions and parameter values (see the third column of Table 1). We established that the simulated tissue exhibits characteristic dynamics of a cell colony in a monolayer: onset of rapid growth, followed by deceleration until saturation (an approximately constant number of cells over time). Furthermore, we confirmed that this overall pattern is robust to stochastic effects and to initial conditions. These results are presented in detail in Sections 3.1 and 3.2. Next, to explore potential therapeutic approaches that target CSCs, we used our model to investigate how changing parameter values (to represent different modes of therapy) would affect tumor progression. Specifically, we focused on manipulation of proliferation rates and differentiation rates. The results of these simulations are presented in Section 3.3.

3.1. General macroscopic behavior of the model

The typical model simulation reflects population dynamics characteristic of a cell colony in a monolayer (Fig. 3). Over time, the cell population (and each subpopulation, i.e., DCs, proliferating CSCs and non-proliferating CSCs) follows a pattern consisting of three phases. In the initial phase, the population growth is characterized by relatively large fluctuations over time, as expected owing to the small initial number of cells and the probabilistic nature of the model. The intermediate phase of the population growth is well approximated by a parabola (Fig. 4B). We refer to the first (quadratic) coefficient of this parabola as the "macroscopic growth rate" of the cell population. In the final phase, due to the space limitation of the CA model, population growth decelerates up to a state of saturation (referred to as a "quasi-steady-state"), at which the number of cells remains more or less constant with small fluctuations (Fig. 4A). This quasi-steady state was consistently observed in almost all model simulations. The only exceptions occurred sporadically at extreme values of parameters (e.g., an unrealistically high differentiation rate, combined with a very low proliferation rate); in these cases the cell population died out during the early steps of the simulation. We use macroscopic growth rate and the sizes of the different cell populations at saturation to compare the population dynamics resulting from different combinations of parameter values.

3.2. Robustness of macroscopic characteristics of the model to stochastic effects, initial conditions and CA size

We checked whether the sizes of the observed cell populations and the spatial distributions of the cells in quasi-steady state varied in repeated simulations with identical initial conditions,

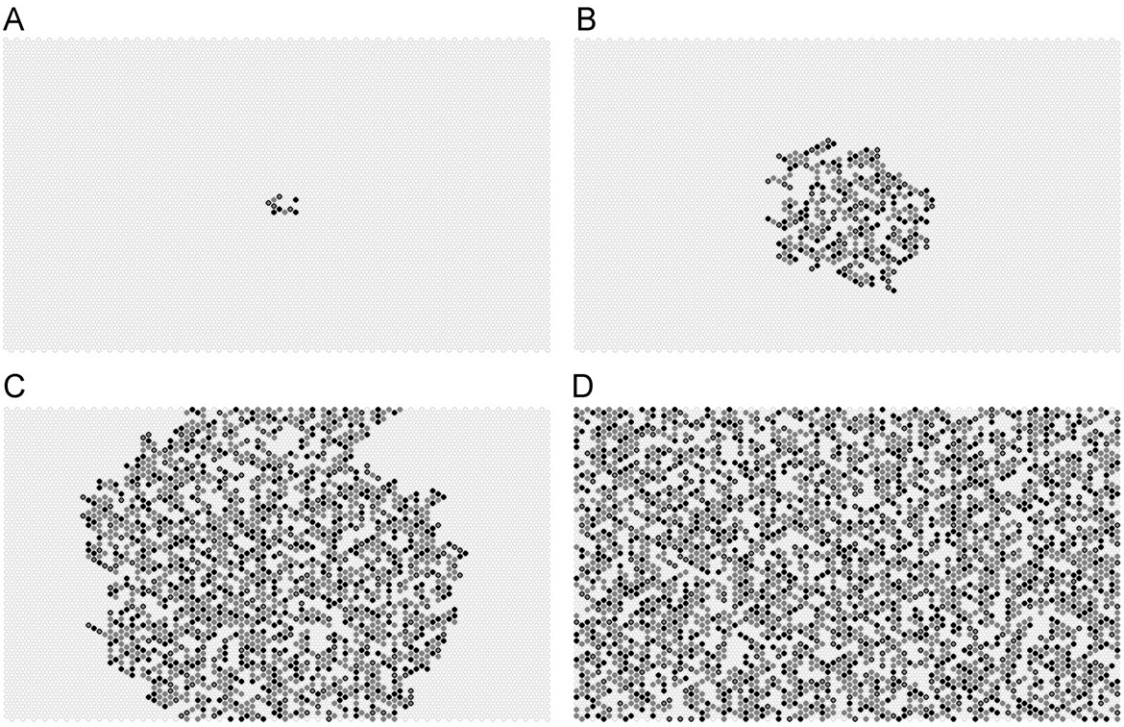

Fig. 3. Examples of model state during the simulation. We show four representative examples of the CA state during the simulation run. Vacant automata cells are marked in yellow, DCs are marked in grey, non-cycling CSCs are represented by black circles, while cycling CSCs are shown as grey circles with a black rim. (A) Initial composition of the model: several cells are present, among them cycling and non-cycling CSCs. (B) Early stages of growth: the colony is small and expands outwards. (C) During later phases, the colony grows more slowly, but still has room to expand. (D) At the final stage, the whole CA is filled and the expansion stops.

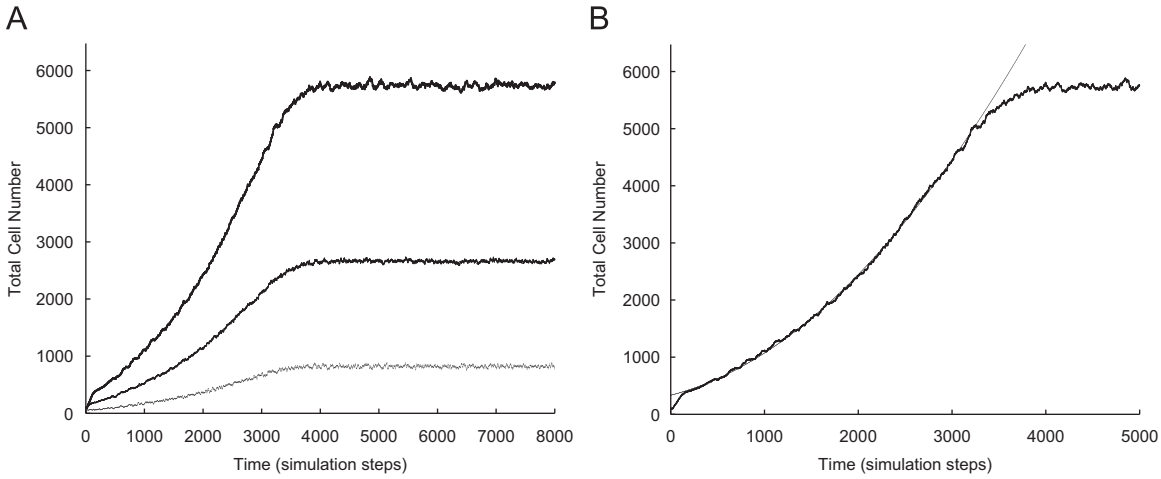

Fig. 4. A representative example of simulation results, showing cell population growth under regular conditions. Initially, 100 cells were seeded in a 20×20 subsquare of the automata. The initial conditions and parameters were set at baseline values (see Table 1). (A) The top curve shows the total number of cells. The intermediate curve shows the total number of CSCs. The bottom curve shows the number of cycling CSCs. The number of cells increases progressively up to a quasi-steady state, where small fluctuations around the threshold are observed. Three phases can be distinguished: initial variable growth, parabolic growth, and decelerated growth up to saturation. (B) The intermediate phase of the cell population growth is well approximated by a parabola (shown by the thin line). The leading coefficient of this parabola is referred to as the "macroscopic growth rate" and is considered as a macroscopic characteristic of the population growth.

Table 2
Model sensitivity to stochastic effects and initial conditions. Relative standard deviation of average values of different stability indices were calculated during the last 1000 time steps of simulations. Panel A: for each one of 13,824 different combinations of initial conditions and parameter values (see Table 1 for specific values) we run 100 simulations for 20,000 time steps; maximal deviations of average values of different cell types are shown. Panel B: for the same simulations as in Panel A, we calculated maximal deviation of the number of neighbors of different cell types of a given cell (i.e., non-cycling CSC neighbors of a DC, DC neighbors of a cycling CSC, etc.). Panel C, sensitivity to initial conditions: for each one of 36 sets of parameter values we run simulations with 240 different initial conditions; maximal deviation of average numbers for different cell types are shown.

Panel A. Model sensitivity to stochastic effects: cell numbers			
All cells	Non-cycling CSCs	Cycling CSCs	DCs
$<0.52\%$	$<0.71\%$	$<0.56\%$	$<0.58\%$
Panel B. Model sensitivity to stochastic effects: mean number of neighbors			
	Non-cycling stem	Cycling stem	Differentiated
	neighbors	neighbors	neighbors
A non-cycling CSC	$<2.29\%$	$<4.08\%$	$<1.12\%$
A cycling CSC	$<3.5\%$	$<10.69\%$	$<1.41\%$
A DC	$<1.15\%$	$<2.46\%$	$<1.34\%$
Panel C. Model sensitivity to initial conditions: cell numbers			
All cells	Non-cycling CSCs	Cycling CSCs	DCs
$<0.5\%$	$<0.72\%$	$<0.56\%$	$<0.55\%$

as well as with different initial conditions and parameter values. As noted above, we performed 100 simulations for each of 13,824 combinations of different initial conditions and parameter values (see the third column of Table 1). The model's quasi-steady state characteristics, namely, mean numbers of cells of each type and mean numbers of neighbors of each type for a given cell, computed over the last 1000 steps of simulation, were insensitive to the initial conditions and to stochastic effects of the simulation (Table 2). We also compared the quasi-steady-state densities of different cell types for different sizes of CA, under the baseline values of the parameters and the baseline initial conditions. We simulated CA of size $\mathbb{Z}_{2n} \times \mathbb{Z}_{2n}$ for each integer value $n \in \{20; 125\}$. The relative cell densities for different cell types and the average ratio between cell number and total number of sites, computed over the last 1000 steps of the simulation, did not depend on the size of the CA (data not shown). The corresponding absolute numbers of cells were proportional to n^2 (i.e., to the number of automata cells).

These results show that the main macroscopic characteristics of the model, such as average densities of cells of different types at quasi-steady state, are insensitive to the initial conditions and to the stochasticity of the model. They depend on the model parameters only, and are scalable to the automata size.

3.3. Controlling tumor progression through different modes of therapy

In order to examine possible ways to control tumor progression by targeting well-defined subpopulations of cancer cells, we investigated relationships between the model parameter values and the growth dynamics of the entire population of cells, represented by the quasi-steady state densities of all cells; of all CSCs and of cycling CSCs; and by the macroscopic growth rate. For each model parameter we sampled six different values within the parameter range, while initial conditions were kept constant (fourth column in Table 1). Initially, we simulated the model varying one of the five parameters, and fixing the other four parameters at the baseline values we defined (second column in Table 1). The results, shown in Figs. 5 and 6, indicate that total cell density and macroscopic growth rate can both be reduced by decreasing the DC lifespan (Figs. 5A and 6A), by decreasing the basic probability of entering the cell cycle (i.e., proliferation rate, Figs. 5B and 6B), or by increasing the probability of differentiation (Figs. 5C,D and 6C,D). However, varying each of these parameters had a different effect on the composition of the cell population. While decreasing the proliferation rate resulted in lower densities of DCs and cycling CSCs (Fig. 5B), decreasing DC lifespan resulted in low DC density but higher cycling CSC density (Fig. 5A). Increasing the maximal differentiation rate or differentiation sensitivity to cell density did not affect densities of DCs and cycling CSCs at all. Rather, each manipulation decreased non-cycling CSC density (Fig. 5C,D). It is important to stress that in all cases, manipulation of a single parameter (while maintaining all other parameters at their "baseline" values) was insufficient to decrease densities of all cell types.

Next, we performed simulations with all possible combinations of the parameter values we sampled (fourth column in Table 1). We found that the effects of each parameter were

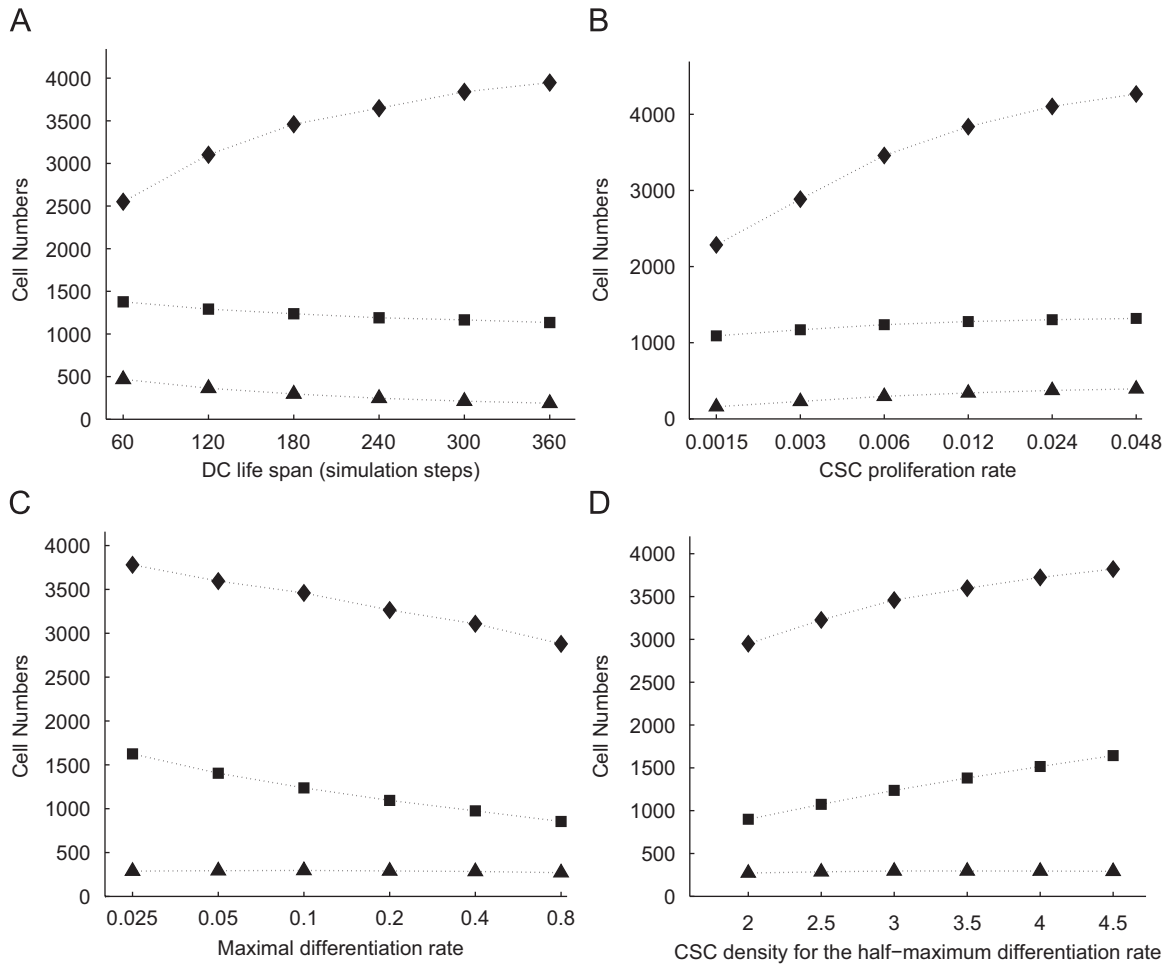

Fig. 5. Dependence of cell populations in the quasi-steady state on model parameters. The cell numbers at the quasi-steady state are plotted as a function of different values of DC lifespan (A), CSC proliferation rate (B), maximal differentiation rate (C), and CSC density giving the half-maximal differentiation rate (D). All other parameters were set at baseline values. Total cell number is represented by rhombuses; total CSC number – by rectangles; cycling CSC number – by triangles.

essentially independent of the other parameters. This means, for example, that regardless of the values of the other parameters, reducing the CSC proliferation rate always resulted in smaller populations of cycling CSC and DCs and in a lower macroscopic growth rate, but it did not affect the size of the non-cycling CSC population. Similar independence was observed for the effects of the other three parameters. The observed effects of the various parameters are summarized in Table 3.

Fig. 7 illustrates the independence of the effects of the various parameters, and the possible implications of this independence for cancer therapy. Fig. 7A shows that decreasing the proliferation rate results in a substantial decrease of the number of cycling CSCs, while this cell population is almost unaffected by changes to the maximal differentiation rate. Conversely, Fig. 7B shows that the size of the non-cycling CSC population is strongly dependent on the maximal differentiation rate but not on the proliferation rate. Taken together, these results indicate that in order to effectively reduce the size of the entire CSC population and to approach cancer eradication, it is insufficient to target proliferation or differentiation alone. Rather, it is necessary to simultaneously promote differentiation and inhibit proliferation (Fig. 7C,D).

4. Discussion

The CSC hypothesis (Sell, 2004) suggests that an efficient anticancer treatment should eliminate as many CSCs as possible (both cycling and non-cycling), while "non-stem" (i.e., differentiated) tumor cells will eventually die out even without intervention. To examine potential approaches towards achieving CSC eradication, we developed a mathematical model of tumor progression, implemented as a probabilistic CA. The model emphasizes the distinction between CSCs and DCs and assumes that CSC fate is governed by quorum sensing, i.e., the ability of a stem cell to "decide" whether to differentiate, on the basis of the number of stem cells in its neighborhood. Our model is simple, relying on only two assumptions concerning local cell behavior: (i) higher total cell density in the microenvironment inhibits cell proliferation, and (ii) higher CSC density in the microenvironment promotes differentiation. In other words, the primary mechanism driving CSC dynamics is QS. A QS mechanism is known to exist in bacteria (Tu et al., 2010), and the existence of QS in CSCs has been both theoretically and experimentally supported (Kirnasovsky et al., 2008b; Agur et al., 2010).

We examined how different forms of therapy, implemented by varying the values of model parameters, affect tumor growth rate and cell population sizes. Three biologically important observations emerged. First, accelerated death of DCs (represented in the model by decreased lifespan) decreased the number of DCs, but increased the number of cycling CSCs (see Fig. 5A). This increase occurred because the accelerated removal of DCs from the population weakened the negative feedback that these cells posed on CSC proliferation. The effect is consistent with the results of Agur et al. (2010), who assumed the existence of a similar local feedback mechanism, and with those of Enderling et al. (2009a)

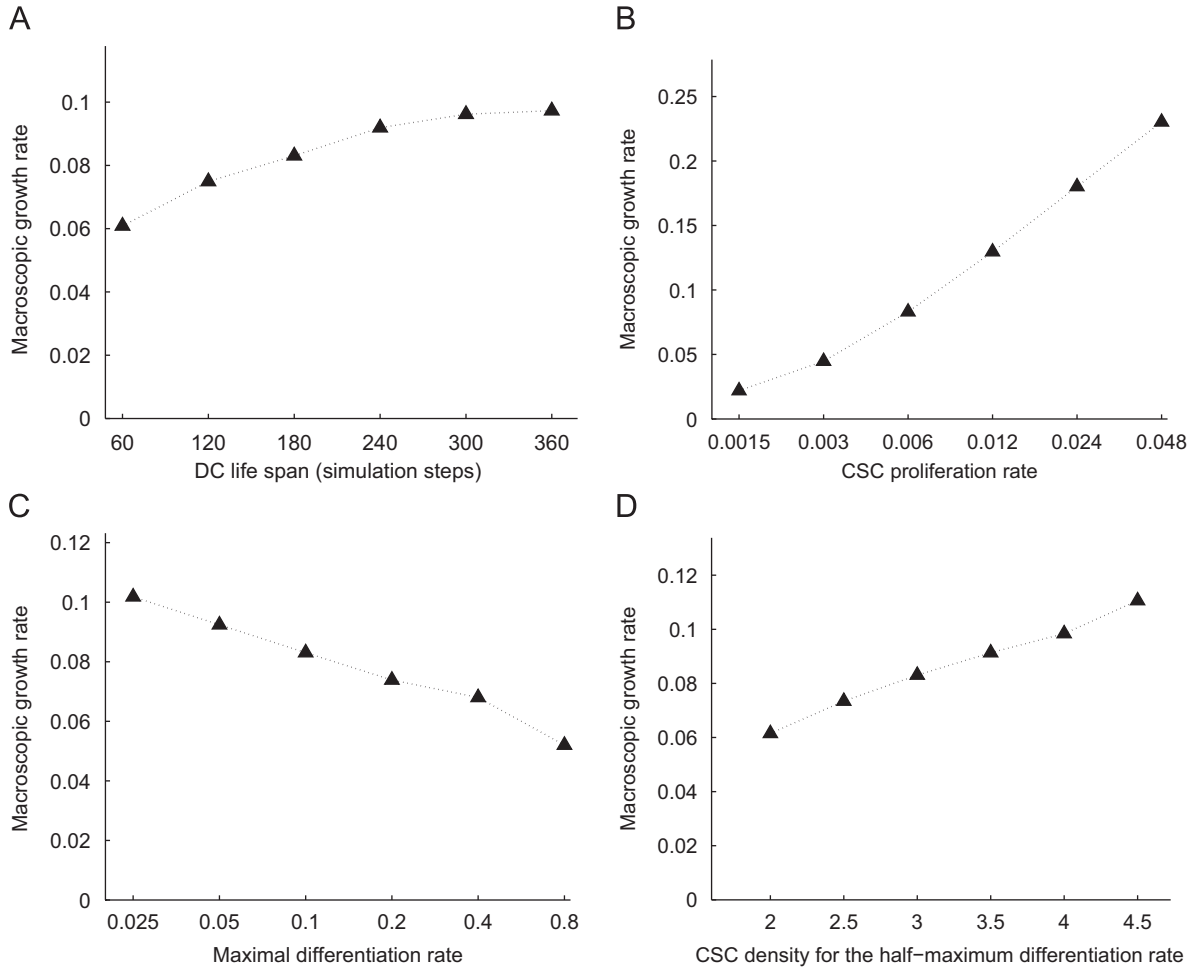

Fig. 6. Dependence of the macroscopic growth rate on model parameters. We show the macroscopic growth rate as a function of DC lifespan (A), CSC proliferation rate (B), CSC maximal differentiation rate (C) and CSC density giving the half-maximal differentiation rate (D). In each case, all other parameters were set at baseline values. The dependence of macroscopic growth rate on model parameters is similar to that of total cell density; see Fig. 5.

Table 3
Summary of the effect of varying model parameters on the macroscopic growth rate and all population sizes. Up arrow means increasing effect of the parameter, down arrow means decreasing effect, "NE" stands for "No Effect". It can be seen that no single parameter change can reduce both cycling and non-cycling CSC density.

Type of intervention	Cycling CSC density	Non-cycling CSC density	DC density	Macroscopic growth rate
Reducing DC lifetime	↑	NE	↓	↓
Reducing proliferation rate	↓	NE	↓	↓
Increasing differentiation	NE	↓	NE	↓

and of Dingli and Michor (2006), who relied on different assumptions. Second, decreasing the proliferation rate of CSCs led to a lower number of cycling CSCs, but the number of non-cycling CSCs remained unchanged (see Fig. 5B). This result is not self-evident, since non-cycling CSCs are produced by proliferation, and inhibition of the latter process might be expected to reduce their number. Third, promoting differentiation (either by increasing the maximal differentiation rate or by increasing the sensitivity of the CSCs to their density) decreased the number of non-cycling CSCs but did not affect the numbers of cycling CSCs and DCs (Fig. 5C, D). Taken together, these results suggest that for a wide range of model parameters, neither inhibition of proliferation alone nor induction of differentiation alone suffices to reduce the number of both cycling and non-cycling CSCs. However, the combination of these two strategies can effectively minimize both populations of CSCs and the total number of cancer cells (Fig. 7).

Our model's assumptions differ from those of other models of CSC dynamics, which either do not consider differentiation as a process triggered by environmental feedback (e.g., Enderling et al., 2009a), or do not take into account the influence of neighboring cells on the differentiation decision (e.g., Bankhead et al., 2007). Still, our observation that effective therapy must specifically target CSCs (i.e., by altering proliferation and differentiation processes) and that killing non-CSCs is ineffective and even detrimental is consistent with the main conclusions of numerous other CSC modeling endeavors that relied on different approaches and assumptions (Dingli and Michor, 2006; Boman et al., 2007; Enderling et al., 2009a; Sottoriva et al., 2010; Zhu et al., 2011). For example, Dingli and Michor (2006) found that the only effective strategies are complete cessation of CSC reproduction or targeted CSC elimination. Boman et al. (2007) suggested that treatment should reduce symmetric division of CSCs, a process equivalent to promoting differentiation. Our analysis suggests that, in view of the fact that in the clinic it is nearly impossible to achieve absolute efficacy with either approach, combining anti-proliferation and differentiation therapy is necessary for effective targeting of CSCs. The simplicity of our model contributes to the generality of our results; they are not restricted by the types of specific assumptions that characterize other

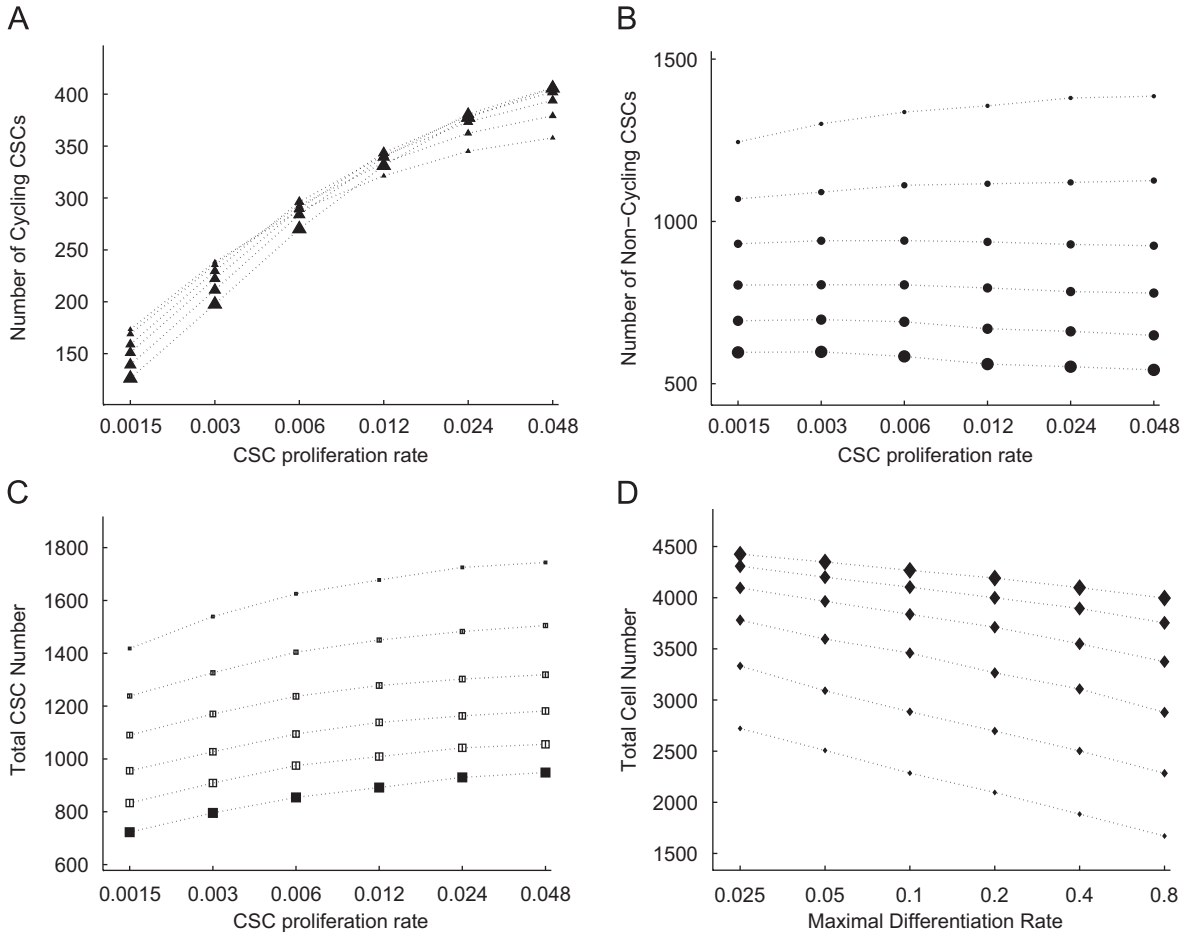

Fig. 7. Dependence of cell population sizes on simultaneous effects of differentiation rate and CSC proliferation rate. (A) Number of cycling CSCs as a function of CSC proliferation rate, for different values of the maximal differentiation rate (distinguished by triangles of different sizes). The sizes of the triangles correspond, respectively, to the differentiation rate values shown in Table 1: the largest triangle corresponds to the highest differentiation rate (0.8), and so on. (B) Number of non-cycling CSCs as a function of proliferation rate, when different values are used for the maximal differentiation rate (distinguished by circles of different sizes, corresponding to the differentiation rate values denoted in Table 1). (C) Total number of CSCs (cycling and non-cycling) as a function of proliferation rate, when different values are used for maximal differentiation rate. (D) Total number of cells (CSCs and DCs) as a function of maximal differentiation rate, when different values are used for CSC proliferation rate. A high maximal differentiation rate combined with a low proliferation rate minimizes the number of CSCs and the total number of cells.

models of CSC dynamics (e.g., assumptions regarding general tumor growth dynamics, population composition, or spatial structure).

Our results provide new insight into some of the disappointing outcomes of clinical trials targeting CSCs. Owing to the low efficacy of cytotoxic therapy on this cell population, research efforts have been invested in the development of differentiation therapy. Yet clinical trials with differentiating agents as monotherapy have failed so far to show clinical benefit despite promising results in vitro. We demonstrate that under a wide range of biologically plausible conditions, differentiation therapy is expected to be ineffective when used alone to eradicate a CSC population, and is only effective in combination with antiproliferative agents. Although it may seem unsurprising that the two treatment approaches are synergistic in eradication of CSCs, our results are notable in showing that combination therapy is a necessary condition for successful cancer treatment.

This finding has profound implications regarding clinical trials of differentiation agents. Thus far, the majority of such trials have been performed without addition of chemotherapy. Moreover, in the case of neuroblastoma, it was even concluded that there would be no utility in continuing to invest in retinoic acid (a differentiating agent) as a potential drug for treatment of the disease, on the basis of two trials that did not incorporate chemotherapy (Adamson et al., 2007). A separate trial, in contrast, later showed a clear benefit when retinoic acid was added to the chemotherapy regimen (Matthay et al., 2009). These observations are further corroborated by clinical experience with acute promyelocytic leukemia, in which administration of a differentiation agent (all-trans retinoic acid) together with antiproliferative agents such as daunorubicin was shown to be efficacious (Rowe and Tallman, 2009). In addition, arsenic trioxide is efficient as a monotherapy in this patient population, possibly due to its dual effect on leukemic cells (both differentiation induction and proliferation inhibition) (Mathews et al., 2006).

In addition, our findings lend perspective to a well-known phenomenon in cancer treatment, in which drugs that seem effective in early studies in terms of "tumor response" later fail due to rapid relapses. We observed that a decrease in macroscopic tumor growth does not necessarily correlate with a decrease in CSC number: for example, a shorter DC lifespan decelerates tumor growth but concomitantly increases CSC densities. This CSC-enrichment effect can explain why tumor regrowth after reduction by chemotherapy can be faster than initial "natural" tumor progression.

Our study provides a compelling theoretical basis for clinical observations of inefficacy of differentiation therapy as a single anticancer treatment. We propose that the effect of differentiating agents should only be assessed in combination with antiproliferative drugs. Otherwise the benefit of these agents can easily be missed.

Acknowledgments

This work was supported by grant #012930 from the NEST FP6 program and by the Chai Foundation. We thank Karen Marron for editing the manuscript and for her helpful advice.

References

Abbott, L.H., Michor, F., 2006. Mathematical models of targeted cancer therapy. Br. J. Cancer 95, 1136–1141.

Adams, J.M., Strasser, A., 2008. Is tumor growth sustained by rare cancer stem cells or dominant clones? Cancer Res. 68 (11), 4018–4021.

Adamson, P.C., Matthay, K.K., O'Brien, M., Reaman, G.H., Sato, J.K., Balis, F.M., 2007. A phase 2 trial of all-trans-retinoic acid in combination with interferon-alpha2a in children with recurrent neuroblastoma or Wilms tumor: A Pediatric Oncology Branch. NCI and Children's Oncology Group Study. Pediatr. Blood Cancer 49 (5), 661–665.

Agur, Z., Daniel, Y., Ginosar, Y., 2002. The universal properties of stem cells as pinpointed by a simple discrete model. J. Math. Biol. 44, 79–86.

Agur, Z., Kogan, Y., Levi, L., Harrison, H., Lamb, R., Kirnasovsky, O.U., Clarke, R.B., 2010. Disruption of a Quorum sensing mechanism triggers tumorigenesis: a simple discrete model corroborated by experiments in mammary cancer stem cells. Biol. Direct 5.

Ashkenazi, R., Jackson, T.L., Dontu, G., Wicha, M.S., 2007. Breast cancer stem cells-research opportunities utilizing mathematical modeling. Stem Cell Rev. 3 (2), 176–182.

Bankhead, A., Magnuson, N.S., Heckendorn, R.B., 2007. Cellular automaton simulation examining progenitor hierarchy structure effects on mammary ductal carcinoma in situ. J. Theor. Biol. 246, 491–498.

Boman, B.M., Huang, E., 2008. Human colon cancer stem cells: a new paradigm in gastrointestinal oncology. J. Clin. Oncol. 26 (17), 2828–2838.

Boman, B.M., Wicha, M.S., Fields, J.Z., Runquist, O.A., 2007. Symmetric Division of Cancer Stem Cells – a Key Mechanism in Tumor Growth that should be Targeted in Future Therapeutic Approaches. Clin. Pharmacol. Ther. 81 (6), 893–898.

Clarke, R.B., Anderson, E., Howell, A., Potten, C.S., 2003. Regulation of human breast epithelial stem cells. Cell Prolif. 36 (Suppl 1), 45–58.

Cortes-Dericks, L., Carboni, G.L., Schmid, R.A., Karoubi, G., 2010. Putative cancer stem cells in malignant pleural mesothelioma show resistance to cisplatin and pemetrexed. Int. J. Oncol. 37 (2), 437–444.

Culine, S., Kramar, A., Droz, J.P., Theodore, C., 1999. Phase II study of all-trans retinoic acid administered intermittently for hormone refractory prostate cancer. J. Urol. 161 (1), 173–175.

d'Onofrio, A., Tomlinson, I.P.M., 2007. A nonlinear mathematical model of cell turnover, differentiation and tumorigenesis in the intestinal crypt. J. Theor. Biol. 244, 367–374.

Dingli, D., Michor, F., 2006. Successful therapy must eradicate cancer stem cells. Stem Cells. 24 (12), 2603–2610.

Dingli, D., Traulsen, A., Michor, F., 2007. (A)Symmetric stem cell replication and cancer. PLoS Comput. Biol. 3 (3).

Enderling, H., Anderson, A.R., Chaplain, M.A., Beheshti, A., Hlatky, L., Hahnfeldt, P., 2009a. Paradoxical dependencies of tumor dormancy and progression on basic cell kinetics. Cancer Res. 69 (22), 8814–8821.

Enderling, H., Hlatky, L., Hahnfeldt, P., 2009b. Migration rules: tumours are conglomerates of self-metastases. Br. J. Cancer 100, 1917–1925.

Enderling, H., Hlatky, L., Hahnfeldt, P., 2010. Tumor morphological evolution: directed migration and gain and loss of the self-metastatic phenotype. Biol. Direct 5 (23).

Flake, A.W., 2004. The conceptual application of systems theory to stem cell biology: a matter of context. Blood Cells Mol. Dis. 32 (1), 58–64.

Ganguly, R., Puri, I.K., 2006. Mathematical model for the cancer stem cell hypothesis. Cell Prolif. 39 (1), 3–14.

Iida, K., Kawai, K., Hayashi, H., Sekido, N., Miyanaga, N., Takeshima, H., Akaza, H., 1999. Cases of refractory testicular cancer treated with all trans-retinoic acid. Gan To Kagaku Ryoho 26 (6), 841–844.

Johnston, M.D., Edwards, C.M., Bodmer, W.F., Maini, P.K., Chapman, S.J., 2007. Mathematical modeling of cell population dynamics in the colonic crypt and in colorectal cancer. Proc. Natl. Acad. Sci. USA 104, 4008–4013.

Kakarala, M., Wicha, M.S., 2008. Implications of the cancer stem-cell hypothesis for breast cancer prevention and therapy. J. Clin. Oncol. 26 (17), 2813–2820.

Kavalerchik, E., Goff, D., Jamieson, C.H., 2008. Chronic myeloid leukemia stem cells. J. Clin. Oncol. 26 (17), 2911–2915.

Kelly, P.N., Dakic, A., Adams, J.M., Nutt, S.L., Strasser, A., 2007. Tumor growth need not be driven by rare cancer stem cells. Science 317 (5836), 337.

Kirnasovsky, O.U., Kogan, Y., Agur, Z., 2008a. Resilience in stem cell renewal: development of the Agur–Daniel–Ginossar model. Disc. Cont. Dyn. Syst. 10, 129–148.

Kirnasovsky, O.U., Kogan, Y., Agur, Z., 2008b. Analysis of a mathematical model for the molecular mechanism of fate decision in mammary stem cells. Math. Mod. Nat. Phenom. 3, 78–89.

Kirouac, D.C., Madlambayan, G.J., Yu, M., Sykes, E.A., Ito, C., Zandstra, P.W., 2009. Cell–cell interaction networks regulate blood stem and progenitor cell fate. Mol. Syst. Biol. 5, 293.

le Viseur, C., Hotfilder, M., Bomken, S., Wilson, K., Rottgers, S., Schrauder, A., Rosemann, A., Irving, J., Stam, R.W., Shultz, L.D., Harbott, J., Jurgens, H., Schrappe, M., Pieters, R., Vormoor, J., 2008. In childhood acute lymphoblastic leukemia, blasts at different stages of immunophenotypic maturation have stem cell properties. Cancer Cell. 14 (1), 47–58.

Lipponen, P., 1999. Apoptosis in breast cancer: relationship with other pathological parameters. Endocr. Relat. Cancer 6, 13–16.

Mathews, V., George, B., Lakshmi, K.M., Viswabandya, A., Bajel, A., Balasubramanian, P., Shaji, R.V., Srivastava, V.M., Srivastava, A., Chandy, M., 2006. Single-agent arsenic trioxide in the treatment of newly diagnosed acute promyelocytic leukemia: durable remissions with minimal toxicity. Blood 107, 2627–2632.

Matthay, K.K., Reynolds, C.P., Seeger, R.C., Shimada, H., Adkins, E.S., Haas-Kogan, D., Gerbing, R.B., London, W.B., Villablanca, J.G., 2009. Long-term results for children with high-risk neuroblastoma treated on a randomized trial of myeloablative therapy followed by 13-cis-retinoic acid: a children's oncology group study. J. Clin. Oncol. 27 (7), 1007–1013.

Michor, F., Nowak, M.A., Frank, S.A., Iwasa, Y., 2003. Stochastic elimination of cancer cells. Proc. R. Soc. London B 270, 2017–2024.

Moreira, J., Deutsch, A., 2002. Cellular automaton models of tumor development: a critical review. Adv. Complex Syst. 5, 247–267.

Pohl, A., Lurje, G., Kahn, M., Lenz, H.J., 2008. Stem cells in colon cancer. Clin. Colorectal Cancer 7 (2), 92–98.

Quintana, E., Shackleton, M., Sabel, M.S., Fullen, D.R., Johnson, T.M., Morrison, S.J., 2008. Efficient tumour formation by single human melanoma cells. Nature 456 (7222), 593–598.

Rowe, J.M., Tallman, M.S., 2009. Therapy for acute myeloid leukemia. In: Hoffman, et al.(ed.), Hematology, New York.

Salmon, S.E., Sartorelli, A.C., 2001. Cancer chemotherapy. In: Katzung, B.G. (Ed.), Basic and Clinical Pharmacology, International Edition. Lange Medical Books/McGraw-Hill, pp. 923–1044.

Sanchez-Garcia, I., Vicente-Duenas, C., Cobaleda, C., 2007. The theoretical basis of cancer-stem-cell-based therapeutics of cancer: can it be put into practice? Bioessays 29 (12), 1269–1280.

Sell, S., 2004. Stem cell origin of cancer and differentiation therapy. Crit. Rev. Oncol. Hematol. 51, 1–28.

Sinicrope, F.A., Hart, J., Hsu, H., Lemoine, M., Michelassi, F., Stephens, L.C., 1999. Apoptotic and mitotic indices predict survival rates in lymph node-negative colon carcinomas. Clin. Cancer Res. 5, 1793–1804.

Sottoriva, A., Verhoeff, J.J.C., Borovski, T., McWeeney, S.K., Naumov, L., Medema, J.P., Sloot, P.M.A., Vermeulen, L., 2010. Cancer stem cell tumor model reveals invasive morphology and increased phenotypical heterogeneity. Cancer Res. 70 (1), 46–56.

Spira, A.I., Carducci, M.A., 2003. Differentiation therapy. Curr. Opin. Pharmacol. 3 (4), 338–343.

Studer, U.E., Jenzer, S., Biedermann, C., Chollet, D., Kraft, R., von Toggenburg, H., Vonbank, F., 1995. Adjuvant treatment with a vitamin A analogue (etretinate) after transurethral resection of superficial bladder tumors. Final analysis of a prospective, randomized multicenter trial in Switzerland. Eur. Urol. 28 (4), 284–290.

Tomasson, M.H., 2009. Cancer stem cells: a guide for skeptics. J. Cell Biochem. 106 (5), 745–749.

Tomlinson, I.P.M., Bodmer, W.F., 1995. Failure of programmed cell death and differentiation as causes of tumors: Some simple mathematical models. Proc. Natl. Acad. Sci. USA 92, 11130–11134.

Trump, D.L., Smith, D.C., Stiff, D., Adedoyin, A., Day, R., Bahnson, R.R., Hofacker, J., Branch, R.A., 1997. A phase II trial of all-trans-retinoic acid in hormone-refractory prostate cancer: a clinical trial with detailed pharmacokinetic analysis. Cancer Chemother. Pharmacol. 39 (4), 349–356.

Tu, K.C., Long, T., Svenningsen, S.L., Wingreen, N.S., Bassler, B.L., 2010. Negative feedback loops involving small regulatory RNAs precisely control the Vibrio harveyi quorum-sensing response. Mol. Cell 37, 567–579.

van Leeuwen, I.M.M., Edwards, C.M., Ilyas, M., Byrne, H.M., 2007. Towards a multiscale model of colorectal cancer. World J. Gastroenterol. 13 (9), 1399–1407.

Zhou, B.B., Zhang, H., Damelin, M., Geles, K.G., Grindley, J.C., Dirks, P.B., 2009. Tumour-initiating cells: challenges and opportunities for anticancer drug discovery. Nat. Rev. Drug Discov. 8 (10), 806–823.

Zhu, X., Zhou, X., Lewis, M.T., Xia, L., Wong, S., 2011. Cancer stem cell, niche and EGFR decide tumor development and treatment response: a bio-computational simulation study. J. Theor. Biol. 269, 138–149.